Supplementary Materials to

Caveats of the isotopic paleothermometer: spatial and temporal isotope – temperature relationships

Mathieu Casado[1], Adriana Bailey[2], Christophe Leroy-Dos Santos[1], Elise Fourré[1], Vincent Favier[3], Cécile Agosta[1], Christoph Kittel[4], Laurent Arnaud[3], Frédéric Prié[1], Pete D. Akers[5], Alexandre Cauquoin[6], Martin Werner[7], Leoni Janssen[1], Barbara Stenni[8], Giuliano Dreossi[8], Andrea Spolaor[8,9], Agnese Petteni[1,2], Joel Savarino[3], Amaelle Landais[1]

This PDF file includes:

Supplementary text S1 to S4
Figures S1 to S4
References (1 to 13)

S1. *Focus on temporal variability in coastal regions*

From 18 November to 22 November, the EAIIST traverse was located at the site of D3, only 5.5 km away from the station DDU, which provides the opportunity for an in-depth comparison of the isotopic composition from two site in immediate proximity. Despite the close proximity, the sites of D3 and DDU are very different. DDU is located at 33 m a.s.l. on a rocky island surrounded by sea ice at the time of the traverse, but which can be open water in summer. In contrast, the D3 site is located at an altitude of 93 m a.s.l. on a blue ice slope 500m away from the coast on the actual continent.

During this period of five days, we observe at both sites two contrasting periods of diurnal variability. On 18–19 November, a weak diurnal cycle of temperature and humidity levels leads to almost no obvious isotopic variability, but the period 19–22 November has large diurnal cycles of temperature and wind speed that are associated with substantial humidity and water isotopic cycles (Fig. S1). Overall, temperature records show parallel diurnal cycles, with a significant offset of 1.1°C ($p < 0.005$ from a non-parametric one-way ANOVA test), partly due to the altitude difference (a dry adiabatic gradient of roughly -10°C/km would suggest a difference of 0.6°C between both sites). The mixing ratio show almost identical diurnal cycles, but for which the humidity levels are slightly higher at EAIIST (50 ppmv difference on average, $p = 0.02$), despite the temperature being lower. The difference is larger during day time period while the humidity levels at DDU and D3 converge toward the same value during the evenings when katabatic winds occur. For the water isotopes, we expect diurnal cycles (Bréant et al., 2019), for which the origin is not directly associated with the temperature variations due to the change of insolation throughout the day. Coherent $\delta^{18}O$ cycles with no significant average difference ($p = 0.4$) are indeed observed during the period from 18 November to 22 November, despite the statistically significant temperature difference.

The measurements of the moisture isotopic composition at these two nearby locations provide key elements to evaluate the impact of the origin of the air masses on the isotopic composition in Polar coastal areas such as Adélie Land. Indeed, Figure S1 shows a significant impact of wind speed on the moisture isotopic composition, with periods of high wind speed (5 $m.s^{-1}$, red and blue shaded periods in Fig. S1) characterised by medium to low mixing ratio and lower $\delta^{18}O$ particularly during katabatic winds (down to -45‰, blue shaded in Fig. S1). Wind directions are unfortunately unavailable for these periods due to malfunction of the AWS sensors, but the katabatic identity is assigned based on known previous katabatic wind timing (Bréant et al., 2019). In order to explain the wide isotopic difference observed for the red (18/11 to 19/11) and blue (19/11 to 22/11) periods despite similar ranges of wind speed and temperature, we made use of air mass back-trajectories (see Methods). As displayed in Figure 2.f), the period from 18 November to 19 November is characterised by a synoptic event during which moisture is transported to Dumont D'Urville along the coast of Victoria and Adélie Lands, whereas from 19 November to 22 November, air masses are advected toward Dumont d'Urville during intense katabatic winds starting around 12:00 UTC and ending around 23:00 UTC coming from the Plateau region.

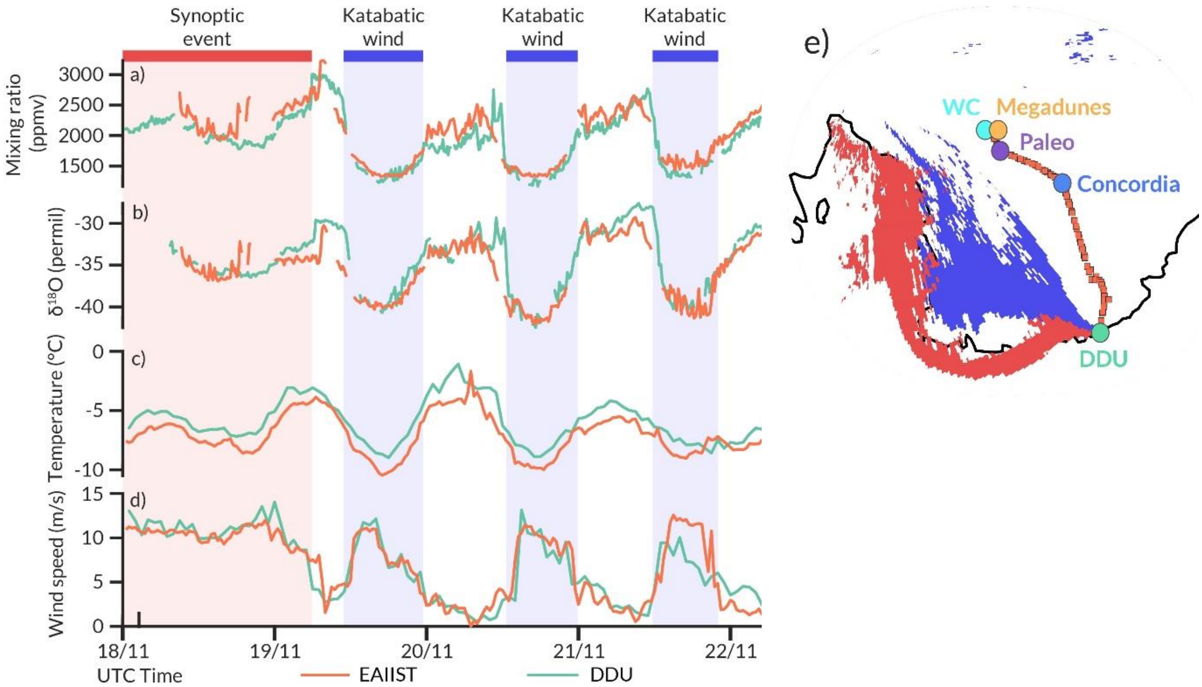

Figure S1: Focus on the isotopic composition diurnal variations in coastal areas: *Timeseries from 18 to 22 November 2019 of a) mixing ratios (ppmv), b) $\delta^{18}O$ (‰), c) temperature from weather stations (°C), d) wind speed (m/s) measured when the EAIIST traverse was at the D3 (orange line), in comparison with data from similar instruments at DDU, 5.5km away (green). The blue shaded areas indicate period with katabatic winds (>5 $m.s^{-1}$) when dry moisture from the continental ice sheet was advected toward DDU and D3, the red shaded area indicates the period during which a synoptic event brought moisture along the coast. e) clusters of back-trajectories during the period from 18/11 to 19/11, characterised by the synoptic event (red) and during the period from 19/11 to 22/11, characterised by katabatic winds (blue).*

S2. *Spatial and temporal variability of isotope and temperature at the synoptic scale*

From 1 December 2019 to 30 January 2020, the EAIIST traverse travelled across the East Antarctic Plateau. The meteorological conditions, and in particular the temperature, during this traverse were extremely similar to Dome C observations (normalised (1SD) RMS difference of temperatures below 0.8 over the entire period). Despite the similar temperature, we observed substantial differences in isotopic composition between the caravan and Dome C over the same period (normalised RMS difference of 3.2 for $\delta^{18}O$). Here, we delve into the difference between the vapour isotopic composition for different regions of the Plateau with similar climate.

When the traverse reached the plateau, it moved toward Concordia station and then continued further south toward the Megadunes area. Temperature and humidity observed on the traverse reached *Antarctic Plateau* conditions (Dome C-like conditions, with an average temperature of ~-35°C and 400ppmv) around 1 December 2019 until 30 January 2020. In contrast, the traverse's vapour $\delta^{18}O$ varied from -50 to -73‰ during this period, while Dome C vapour $\delta^{18}O$ remained bounded between -67 and -70‰, leading to significant differences of vapour $\delta^{18}O$ (up to 20‰) which persists except when the traverse reaches Dome C (4 December and 18 January).

Specifically, we focus on three case studies from stops of the traverse during which we have at least 12 hours of measurement. For each of these periods, the temperature at Dome C and the location of the EAIIST traverse are not significantly different (less than 1°C, $p > 0.05$ from a non-parametric one-way ANOVA test). For all of these periods, we obtain significant differences ($p < 0.05$) between the $\delta^{18}O$ at Dome C and on the EAIIST traverse, even when the distance is as low as 150km. Since the temperatures at both sites were very similar, the difference of water vapour isotopic composition can be linked with either different origin of the air masses, or different mixing in the atmospheric boundary layer.

The history of the air masses before arriving to the traverse or Concordia station was evaluated using the Flexpart Lagrangian model Lagrangian Particle Dispersion Model Flexpart 10 (Pisso et al., 2019). The model as forced using ERA5 hourly data and produced an ensemble of 10 000 back-trajectories with a three-hour timestep for 10 days. The ensemble of trajectories for these virtual particles were then clustered to evaluate the horizontal and vertical past history of the air masses. To do so, we used a threshold on the density of trajectories (defined as the calculation indicates the proportion of particles over the ten-days back-trajectory at each grid point relatively to total amount of particles) to evaluate the areas including the largest ensemble of trajectories.

We produced trajectories ending at the gridpoint of interest at 1000m altitude to be free from the local, small scale vertical mixing near the boundary layer. Yet, since our measurements were taken very much inside the atmospheric boundary layer (between 2 and 5 m above the ground), we also computed as well back-trajectories ending at 50m altitude. The difference, while noticeable, do not affect the qualitative interpretation of the results.

Using back trajectory analysis, we obtain a large range of contrasting vertical and horizontal origin of the air masses from similar horizontal history (Fig. S2a), to no horizontal overlap (Fig. S2e). For the first case, 01 December 2019, despite the proximity of the traverse with Dome C, similar climatic conditions, and similar horizontal air masses history, we observe significant difference in isotopic composition (Fig. S2a). In this case, the air masses were at different altitudes except for the last two days of the air masses history, and despite virtually equal final temperatures, they experience different temperatures for most of the history, and in particular when precipitation took place (6 days prior for the EAIIST traverse, against only 2 days prior for Dome C, Fig. S2b). In the two other cases, different origins with various amount of overlap explain the difference in final isotopic composition, despite again similar temperature. In all these cases, despite similar local conditions, the horizontal or vertical differences in air masses transport could lead to significant isotopic composition.

We also evaluated the stability of the atmospheric boundary layer by calculating the Richardson Number (Richardson, 1920) in the boundary layer using the outputs of the regional model MAR, since it has been shown in Greenland that it can impact the vapour isotopic composition in the atmospheric boundary layer (Berkelhammer et al., 2016). Overall, a much more variable Richardson number is observed at Dome C, with night-time values often larger than 0.25 and negative day-time values, than the other locations covered by EAIIST traverse on the Plateau where the Richardson number remains between 0 and 0.1. This suggests that the boundary layer at Dome C alternated between stable and stratified boundary layer and non-stable convective atmosphere (King et al., 2006) , between night and day, respectively. These conditions, however, do not reflect those observed outside of the Dome which undergo a relatively strong mixing consistently during days and night as suggested by $R_i < 0.1$ (Zilitinkevich et al., 2008). During the six stops of the EAIIST traverse, the conditions at Dome C remained well mixed except during the Paleo stop on 17 December 2019. In this case, enhanced mixing between the boundary layer and the free atmosphere at Paleo could also explain the difference between the boundary layer isotopic composition.

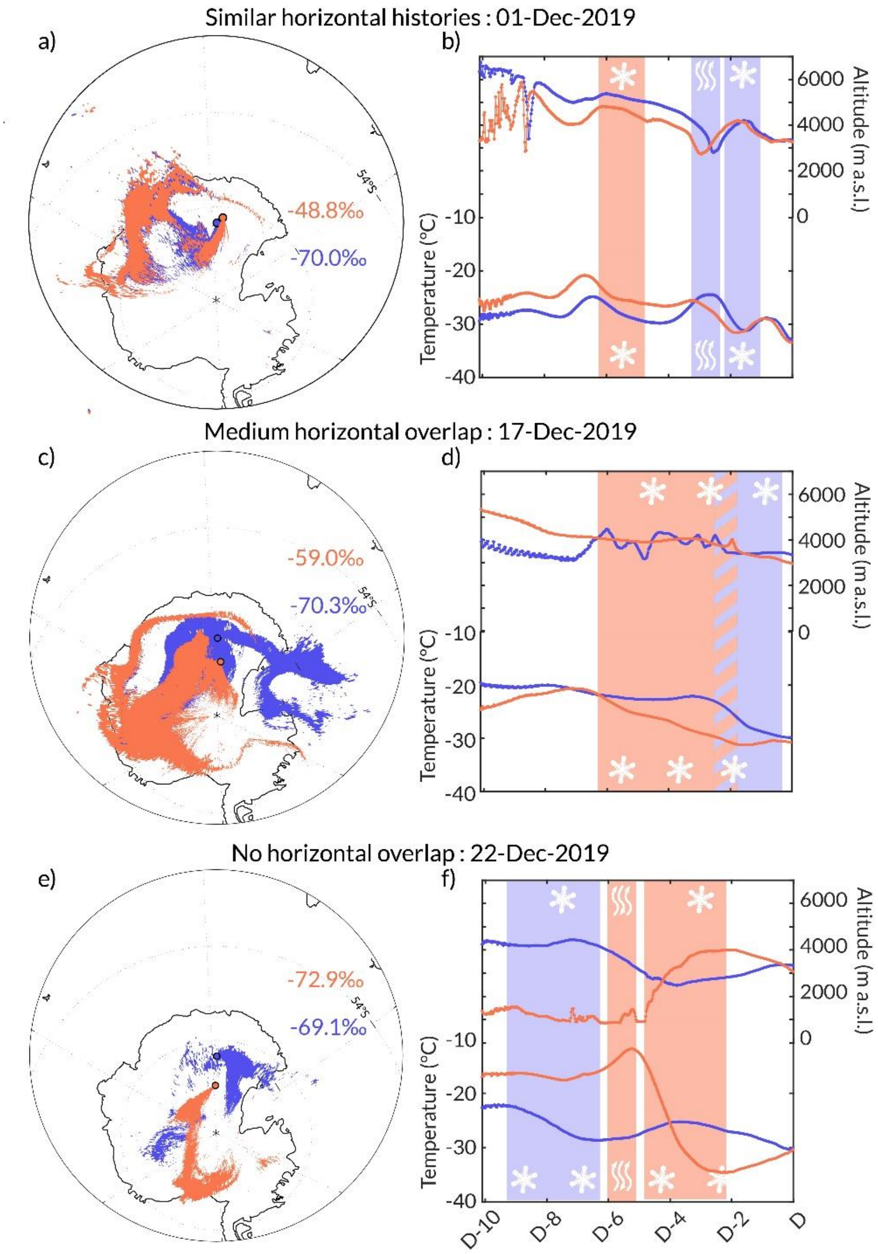

Figure S2: Back-trajectory analyses for stationary periods of the EAIIST traverse: *ensemble of back-trajectories reaching Dome C (Blue) and the location of the EAIIST traverse (orange) for three case studies: a) and b), 1 December, similar horizontal histories, c) and d) 17 December, medium horizontal ofverlap, and e) and f) no horizontal overlap. The average isotopic composition measured at each location is given, as well as the altitude (m a.s.l.) and temperature (°C) as a function of time for both trajectories (b), d), f)).*

These differences in isotopic composition that exist despite similar climatic conditions reinforce that the link between isotopic composition and temperature is more complex than a simple linear regression, even for a place with relatively homogeneous conditions. Overall, the isotope-temperature relationship is calculated by averaging a large ensemble of synoptic conditions, either in the case of the average of several years of snow isotopic composition (Lorius et al., 1969), or long time series of precipitation isotopic composition (Stenni et al., 2017). Yet, this confirms that the link between local temperature and isotopic composition is actually not direct, but comes from the link of both these variables with the temperature gradient along the distillation pathway. As a result, this suggests that we can use the vapour measurements presented in this manuscript as an indicator of large scale Rayleigh distillation pattern at the day-to-day scale, rather than as indicator of only local exchange within the atmospheric boundary layer for which only the local temperature and snow isotopic composition would matter.

S3. Comparison between snow and vapour isotopic composition

To further evaluate whether the vapour isotopic composition variations can be explained by the local exchange with surface snow, we compare at Dome C and across the EAIIST traverse the vapour and snow isotopic composition (Figure S3). There is ample evidence that the vapour isotopic composition diurnal cycle is dominated by sublimation and condensation near the surface with moisture fluxes restricted to the atmospheric boundary layer (Casado et al., 2016, 2018; Ritter et al., 2016; Vignon et al., 2017). Here, at the day-to-day scale, we evaluate the impact of variations of snow isotopic composition on the vapour isotopic composition (Fig. S3a). Over the entire traverse, we observe a relatively good correlation linked with the parallel Rayleigh distillation from the coast to Dome C. On the plateau over the traverse and at Dome C, the correlation is completely destroyed ($r^2 = 0.03$, $p > 0.5$ for EAIIST for snow $\delta^{18}O < 45$‰). This confirms that at the day-to-day scale or spatially over the Antarctic Plateau, the vapour isotopic composition is not controlled directly by the snow isotopic composition.

We evaluated if the isotopic fractionation during sublimation or condensation could be responsible for the difference between the snow and vapour isotopic composition variations on the East Antarctic Plateau by computing the impact of fractionation at the average temperature of the day. We do not find a link between the vapour isotopic composition and the vapour that would be at equilibrium with the snow (Fig. 3b), and the spatial correlation over the Plateau or the temporal correlation at Dome C are not improved with p values remaining above 0.5. We did not take into account kinetic fractionation which are mainly associated with second order impacts on the isotopic composition.

This additional line of evidence suggests that the vapour here is not controlled by the local exchanges with the snow.

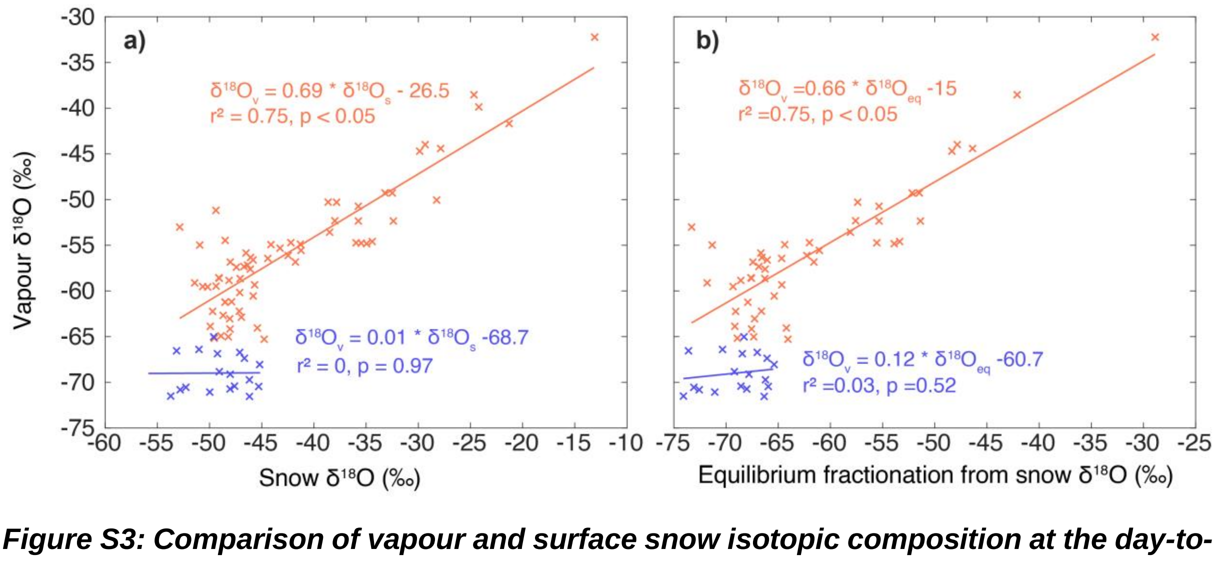

Figure S3: Comparison of vapour and surface snow isotopic composition at the day-to-day scale: *a) vapour and surface snow isotopic composition on EAIIST (orange) and at Dome*

C (blue) during the traverse, b) vapour and calculation of vapour isotopic composition at equilibrium with the surface snow taking into account the average temperature of each day on EAIIST (orange) and at Dome C (blue).

S4. Evaluation of the spatial variability of the temporal and spatial isotope relationships in the model outputs

(Goursaud et al., 2018) showed a strong variability in the isotope-temperature relationship for even nearby gridpoints of GCM outputs in Antarctica. We found similar results here which justify that only qualitative comparison can be made from the model outputs. Figure S4 presents the ensemble of slopes found for the neighbouring gridpoints to Dome C, taking into account the 18 closest gridpoints (± 0.5° latitude, ± 1° longitude, ±10 mbar).

Strong local variability is visible for all regressions, even though, most regression illustrated here were significant. Interestingly, we obtain the same isotope-temperature relationship at Dome C for NDJF, seasonal and interannual timescales, despite the large amplitude of violin plots. There could be a difference due to the dome position of Dome C, which has a different boundary layer dynamic, and for which we could expect a different behaviour than the rest of the Plateau nearby. While there are physical reasons for these difference for neighbouring gridpoints, considering the coarseness of the model outputs, potential missing exchanges between the surface snow and the atmosphere for the vapour isotopic composition, it appears necessary to have a conservative approach and limit the interpretation of the slopes obtained from iso-GCM outputs to ±0.1 ‰.°C^{-1}.

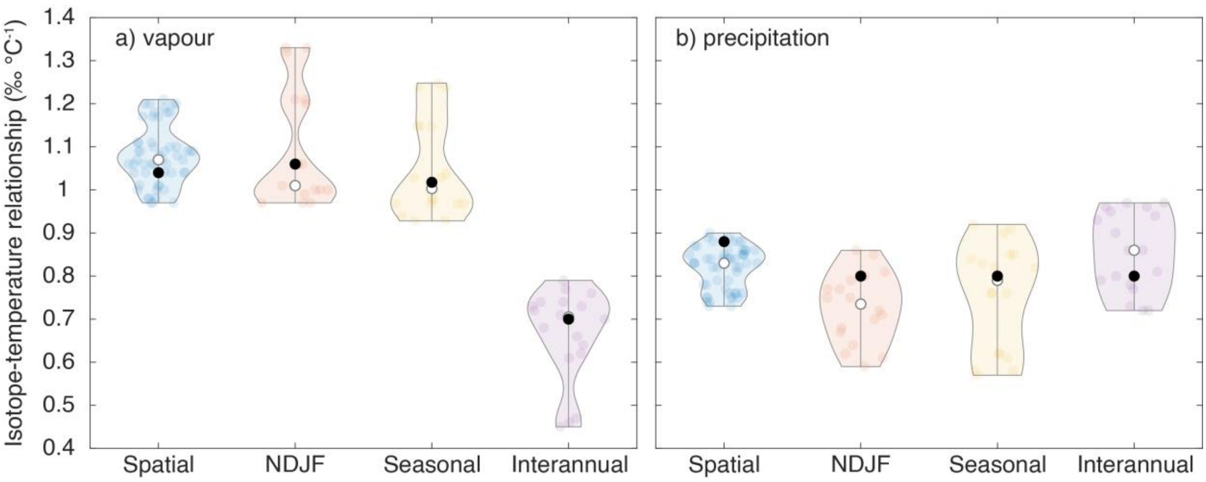

Figure S4: Variability of the isotope-temperature relationships for the neighbouring gridpoints: *a) isotope-temperature slope in the vapour, b) slope in the precipitation for the 18 combinaisons of neighbouring gridpoints (coloured points, note that for spatial relationships, which are obtained by difference between Dome C and Dumont D'Urville, there are more combinaisons because we can combine neighbouring points at both sites), average value (white dot), and nearest gridpoint from Dome C (black dot)*

Bibliography

Berkelhammer, M., Noone, D. C., Steen-Larsen, H. C., Bailey, A., Cox, C. J., O'Neill, M. S., Schneider, D., Steffen, K. and White, J. W. C.: Surface-atmosphere decoupling limits accumulation at Summit, Greenland, Sci. Adv., 2(4), 2016.

Bréant, C., Dos Santos, C. L., Agosta, C., Casado, M., Fourré, E., Goursaud, S., Masson-Delmotte, V., Favier, V., Cattani, O. and Prié, F.: Coastal water vapor isotopic composition driven by katabatic wind variability in summer at Dumont d'Urville, coastal East Antarctica, Earth Planet. Sci. Lett., 514, 37–47, 2019.

Casado, M., Landais, A., Masson-Delmotte, V., Genthon, C., Kerstel, E., Kassi, S., Arnaud, L., Picard, G., Prie, F., Cattani, O., Steen-Larsen, H. C., Vignon, E. and Cermak, P.: Continuous measurements of isotopic composition of water vapour on the East Antarctic Plateau, Atmos. Chem. Phys., 16(13), 8521–8538, doi:10.5194/acp-16-8521-2016, 2016.

Casado, M., Landais, A., Picard, G., Münch, T., Laepple, T., Stenni, B., Dreossi, G., Ekaykin, A., Arnaud, L., Genthon, C., Touzeau, A., Masson-Delmotte, V. and Jouzel, J.: Archival processes of the water stable isotope signal in East Antarctic ice cores, Cryosph., 12(5), 1745–1766, doi:10.5194/tc-12-1745-2018, 2018.

Goursaud, S., Masson-Delmotte, V., Favier, V., Orsi, A. and Werner, M.: Water stable isotope spatio-temporal variability in Antarctica in 1960--2013: observations and simulations from the ECHAM5-wiso atmospheric general circulation model, Clim. Past, 14(6), 923–946, doi:10.5194/cp-14-923-2018, 2018.

King, J. C., Argentini, S. A. and Anderson, P. S.: Contrasts between the summertime surface energy balance and boundary layer structure at Dome C and Halley stations, Antarctica, J. Geophys. Res. Atmos., 111(D2), n/a--n/a, doi:10.1029/2005JD006130, 2006.

Lorius, C., Merlivat, L. and Hagemann, R.: Variation in the mean deuterium content of precipitations in Antarctica, J. Geophys. Res., 74(28), 7027–7031, doi:10.1029/JC074i028p07027, 1969.

Pisso, I., Sollum, E., Grythe, H., Kristiansen, N. I., Cassiani, M., Eckhardt, S., Arnold, D., Morton, D., Thompson, R. L., Groot Zwaaftink, C. D., Evangeliou, N., Sodemann, H., Haimberger, L., Henne, S., Brunner, D., Burkhart, J. F., Fouilloux, A., Brioude, J., Philipp, A., Seibert, P. and Stohl, A.: The Lagrangian particle dispersion model FLEXPART version 10.4, Geosci. Model Dev., 12(12), 4955–4997, doi:10.5194/gmd-12-4955-2019, 2019.

Richardson, L. F.: The Supply of Energy from and to Atmospheric Eddies., 1920.

Ritter, F., Steen-Larsen, H. C., Werner, M., Masson-Delmotte, V., Orsi, A., Behrens, M., Birnbaum, G., Freitag, J., Risi, C. and Kipfstuhl, S.: Isotopic exchange on the diurnal scale between near-surface snow and lower atmospheric water vapor at Kohnen station, East Antarctica, Cryosph., 2016, 1–35, doi:10.5194/tc-2016-4, 2016.

Stenni, B., Curran, M. A. J., Abram, N., Orsi, A., Goursaud, S., Masson-Delmotte, V., Neukom, R., Goosse, H., Divine, D. and Van Ommen, T.: Antarctic climate variability on regional and continental scales over the last 2000 years, Clim. Past, 13, 1609–1634, 2017.

Vignon, E., van de Wiel, B. J. H., van Hooijdonk, I. G. S., Genthon, C., van der Linden, S. J. A., van Hooft, J. A., Baas, P., Maurel, W., Traullé, O. and Casasanta, G.: Stable boundary layer regimes at Dome C, Antarctica: observation and analysis, Q. J. R. Meteorol. Soc., 2017.

Zilitinkevich, S. S., Elperin, T., Kleeorin, N., Rogachevskii, I., Esau, I., Mauritsen, T. and Miles, M. W.: Turbulence energetics in stably stratified geophysical flows: Strong and weak mixing regimes, Q. J. R. Meteorol. Soc., 134(633), 793–799, doi:10.1002/qj.264, 2008.